EXPERIMENT 1

DESIGN OF EXPERIMENTS

1 INTRODUCTION

Engineers frequently encounter complex systems where theoretical models alone are insufficient to predict behaviour, necessitating empirical testing to define processes and identify system characteristics. To effectively characterize these "black box" systems, one must move beyond simple measurement taking and employ a robust Design of Experiments (DOE) methodology. The primary objective of this approach is to maximize the information gained regarding system performance while minimizing the resources and time expended on data collection. This involves a structured conceptual design that transforms vague problem statements into precise statistical inquiries, allowing engineers to detect complex relationships between variables that unstructured testing would miss.

The foundation of any experimental design is System Identification, which treats the process as a system with distinct inputs and outputs. In this framework, variables are classified into three distinct categories to structure the experiment. The first category consists of Controllable Factors (Inputs), which are the independent variables the engineer deliberately manipulates to observe a change. These are often set to specific "levels" (such as low and high) during the experiment. The second category includes the Response Variables (Outputs), which are the measurable performance metrics used to judge the system's behaviour, such as thermal conductivity or vibration amplitude. Finally, the system includes Uncontrollable Factors, often termed "noise," which are external variables like humidity or ambient vibration that affect the system but cannot be easily regulated. Identifying these variables is critical for distinguishing between signal (true process changes) and noise (random error).

A common but flawed approach to experimentation is the One-Factor-at-a-Time (OFAT) method. This method involves holding all factors constant except for one, which is varied to observe its effect on the response. While intuitively simple, OFAT is mathematically inefficient and often misleading because it fails to detect interaction effects. An interaction occurs when the effect of one variable depends on the level of another variable—for instance, if a material only insulates poorly when both temperature is high and pressure is low. OFAT would likely miss this critical "danger zone" by testing pressure and temperature in isolation. Consequently, a robust DOE approach replaces OFAT with a Design Matrix that varies multiple factors simultaneously according to a specific pattern, often using standard notation like -1 (low level) and +1 (high level) to capture these complex interactions.

To ensure the statistical validity of the experimental results, the design must adhere to three fundamental principles: Randomization, Replication, and Blocking.

Randomization is the practice of performing experimental runs in a random order rather than a standard sequence. This technique is essential for averaging out the effects of extraneous factors that may change over time, such as machine warm-up or tool wear. By randomizing the

run order, the experimenter prevents these systematic errors from biasing the results and ensures that observations are statistically independent.

Replication involves repeating the entire experimental condition to estimate the true experimental error. It is crucial to distinguish replication from simple "repetition." Repetition is merely measuring the same sample twice, which only quantifies measurement device consistency. Replication requires resetting the experiment entirely—such as building a new sample or restarting the machine—to capture the variation inherent in the process itself. Without adequate replication, it is impossible to determine if a change in output is due to the controllable factors or simply random process variation.

Blocking is a technique used to improve precision by arranging experiments into homogeneous groups to handle known but nuisance factors. If an experiment must be conducted over two different days or using two different batches of raw material, these differences can introduce significant variability. Blocking allows the experimenter to statistically isolate or "block out" this variability, ensuring that the differences observed in the response variable are driven by the controllable factors rather than the nuisance variable (e.g., the day of testing).

The theoretical framework of DOE is applied to solve specific engineering problems by defining an "Experimental Scope" for various scenarios. Whether optimizing the thermal coating of a UAV, improving the throughput of a food transport system, or reducing vibrations in an off-road vehicle, the process remains consistent. The engineer must select specific Response Variables (y) and Controllable Factors (x) relevant to the case, such as nozzle temperature or spring stiffness, and define a DOE goal. This goal often focuses on identifying non-linear responses or "Optimal Operating Windows" where the system performs best, requiring a design capable of mapping interactions rather than just linear trends.

In this experiment, you are required to design a conceptual experimental setup. You are expected to go beyond simple data collection procedures and demonstrate how the principles of randomization, replication, and blocking are used to identify interactions between variables.

2 CASE STUDIES

Case studies given below are assigned according to the last number of your student ID.

Case Study 1 (0, 5) - Thermal Optimization of UAV Coating:

Background: A start-up is developing a high-altitude Unmanned Aerial Vehicle (UAV) using a proprietary composite material. The material's heat conduction properties are non-linear and sensitive to environmental interactions.

The Problem: You must determine how the thermal conductivity (k) is affected by the interaction of external flight conditions. Simply measuring k at room temperature is insufficient; you must define the process over a specific interval $[x_1, x_2]$.

Experimental Scope:

- **Response Variable (y):** Thermal Conductivity.
- **Controllable Factors (x):** You must investigate at least three factors, such as surface temperature, air pressure and material thickness.
- **DOE Goal:** Determine if there is a significant interaction effect between pressure and temperature. (e.g., Does the material insulate worse at low pressure *only* when the temperature is high?)

Case Study 2 (1, 6)- High-Efficiency Food Transport System:

Background: A food processing plant uses a conveyor system to move delicate packaged goods. The current system suffers from inconsistent throughput due to variable friction, leading to product damage.

The Problem: Management requires a new transport design that optimizes the transport velocity (v) while minimizing the coefficient of friction (μ) to prevent damage.

Experimental Scope:

- **Response Variables (y):** Friction Coefficient (μ).
- **Controllable Factors (x):** You must investigate factors such as conveyor surface texture, product load and belt speed.
- **DOE Goal:** Identify the "Optimal Operating Window." (e.g., Does increasing the speed significantly increase friction due to heat build-up?)

Case Study 3 (2, 7) - Structural Optimization of 3D Printed Aerospace Parts:

Background: An aerospace start-up is using Fused Deposition Modeling (FDM) to manufacture lightweight brackets for drones. However, the printed parts exhibit inconsistent mechanical strength, occasionally failing under loads that theoretical models predict they should withstand.

The Problem: You must determine the optimal printing parameters to maximize the Ultimate Tensile Strength (UTS) without making the print process prohibitively slow.

Experimental Scope:

- **Response Variable (y):** Ultimate Tensile Strength.
- **Controllable Factors (x):** You must investigate at least three factors, such as layer height, nozzle temperature and infill density.
- **DOE Goal:** Determine the interaction effects on layer adhesion. (e.g., Does increasing the nozzle temperature improve strength only when the layer height is small, or does it cause degradation at larger layer heights?)

Case Study 4 (3, 8)- Vibration Isolation in Off-Road Vehicle Suspension:

Background: An ATV manufacturer is designing a new suspension system for rough terrain usage. Drivers have reported excessive fatigue due to high-frequency vibrations being transmitted through the chassis during high-speed manoeuvres.

The Problem: You need to design a suspension setup that minimizes the vertical acceleration transmitted to the driver's seat while maintaining vehicle stability.

Experimental Scope:

- **Response Variable (y):** Vertical acceleration at the seat base (vibration amplitude).
- **Controllable Factors (x):** You must investigate at least three factors, such as spring stiffness, damper oil viscosity, and tire pressure.
- **DOE Goal:** Identify the non-linear damping response. (e.g., Is there a "critical point" where increasing oil viscosity stops reducing vibration and actually starts transmitting *more* shock to the chassis?)

Case Study 5 (4, 9)- Precision Surface Finishing for Medical Implants:

Background: A biomedical engineering firm is manufacturing titanium hip replacements using CNC milling. The surface finish is critical; if it is too rough, it causes excessive wear, but if the machining is too slow, production costs skyrocket.

The Problem: You must characterize the machining process to achieve a specific Surface roughness, avoiding "chatter" (machining vibrations) that ruins the part.

Experimental Scope:

- **Response Variable (y):** Surface roughness.
- **Controllable Factors (x):** You must investigate at least three factors, such as spindle speed (rpm), feed rate, and depth of cut.
- **DOE Goal:** Process stability mapping. (e.g., Does increasing the Depth of Cut trigger unstable chatter vibrations *only* at specific Spindle Speeds, creating a "danger zone" to avoid?)

3 REPORT

The main body of your report must strictly follow the structure below. This structure mirrors the System Identification and Estimation Theory concepts covered in the presentation.

3.1 System Identification (The "Black Box" Model)

Define the system you are testing:

- **Inputs (Factors):** Classify your variables. Which are controllable constants? Which are variables you will manipulate?
- **Outputs (Responses):** What are you measuring to judge performance?
- **Uncontrollable Factors (Noise):** Identify variables (e.g., humidity, vibrations) that act as noise in your "Black Box" model.

3.2 Design Strategy: DOE vs. OFAT

- **Design Matrix:** Create a table showing your experimental runs. Use a standard notation (e.g., Low (-1), High (+1) levels) for your factors.
- **Rejection of OFAT:** Explicitly explain why a One-Factor-at-a-Time approach is unsuitable for this specific problem. Discuss how OFAT would fail to capture the Interactions (e.g., Pressure × Temperature) inherent in your case study.

3.3 Application of Statistical Principles

Explain how you will apply the three pillars of experimental design defined in the lecture:

- **Randomization:** How will you randomize the run order to satisfy the Randomization Principle? Why is this necessary to avoid systematic error?
- **Replication:** Differentiate between "repetition" (measuring the same sample twice) and "replication" (resetting the experiment). How many replications are needed to estimate the experimental error?
- **Blocking:** How will you apply the Blocking Principle to handle nuisance factors? (e.g., If Case 2 experiments take place over two days with different humidity levels, how do you block for "Day"?)

3.4 Experimental Setup

- **Schematic Drawing:** A detailed drawing of your proposed experimental setup.
- **Measurement Devices:** A list of devices needed to measure your Inputs (x) and Outputs (y). Justify why you selected these specific devices (range, sensitivity, cost and availability).
- **Procedure:** A step-by-step guide on how to execute the Design Matrix created in Section 3.2.

4 REFERENCES

1. J. P. Holman, Experimental Methods for Engineers, Eighth Edition, Mc-Graw Hill, 2012.

EXPERIMENT 2

CALIBRATION EXPERIMENT

PURPOSE OF THE EXPERIMENT

To derive the thermocouple calibration curve and equation.

1. INTRODUCTION

Calibration is a set of measurements used to measure the accuracy, determine and document deviations of measurement tool using a known accuracy measurement standard or system under specified conditions. Thanks to the control and calibration of measuring and test equipment, the conformity of the measurements made during production and control is ensured. The continuity of this assurance provided by calibration should be checked from time to time by calibration. The purpose of calibration is to determine and document how much the device or equipment used deviates from the actual value.

2. THEORY

As seen in Figure 1, a closed circuit is formed by joining the ends of two different metals A and B. In this state, if one of the ends is raised to the temperature T1 and the other end is left at a lower temperature T2, an electric current is generated on the metal wire [1]. This phenomenon is known as the Seebeck effect in thermoelectricity. The amount of the current depends on the metals and the temperatures (T1 and T2).

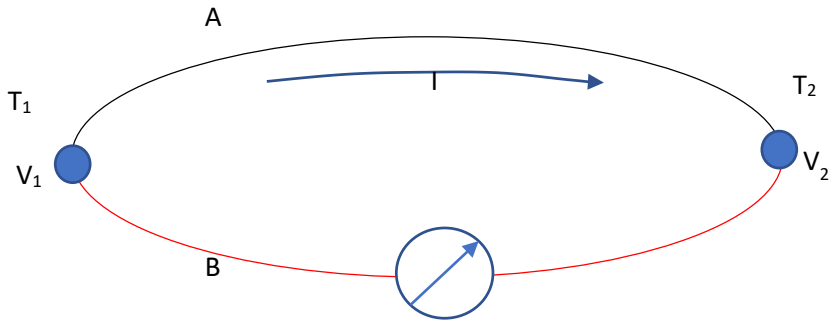

Figure 1. Thermoelectric circuit consisting of A and B wires

When the voltage V_1 is different from the voltage V_2, current occurs. Here, if $T_1 = T_2$, a current will not occur.

The Seebeck effect can be used to measure temperature precisely. The K type thermocouple consists of two different wires containing alloys whose positive pole is Nickel-Chromium (Ni-Cr), and the negative pole is Nickel-Aluminium (Ni-Al). Green wire is positive pole, white wire is negative pole. As shown in Figure 2, when the junctions of the wires are exposed to heat, a voltage of microvolt (μV) is generated between the metal ends, which creates a direct current. The resulting voltage difference is directly proportional to the temperature.

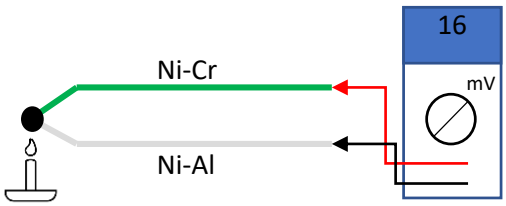

Figure 2. The operating principle of thermocouple

Table 1 shows the thermocouple types, metal types used, measuring range and color codes.

Table 1. Thermocouple types and properties

TYPE	CONDUCTOR TYPE		TEMPERATURE RANGE (°C)	COLOR CODING		
	(+) Lead	(-) Lead		IEC584-3	ANSI/MS/96.1	DN 43714
J	Fe	Cu-Ni	-210 to1200	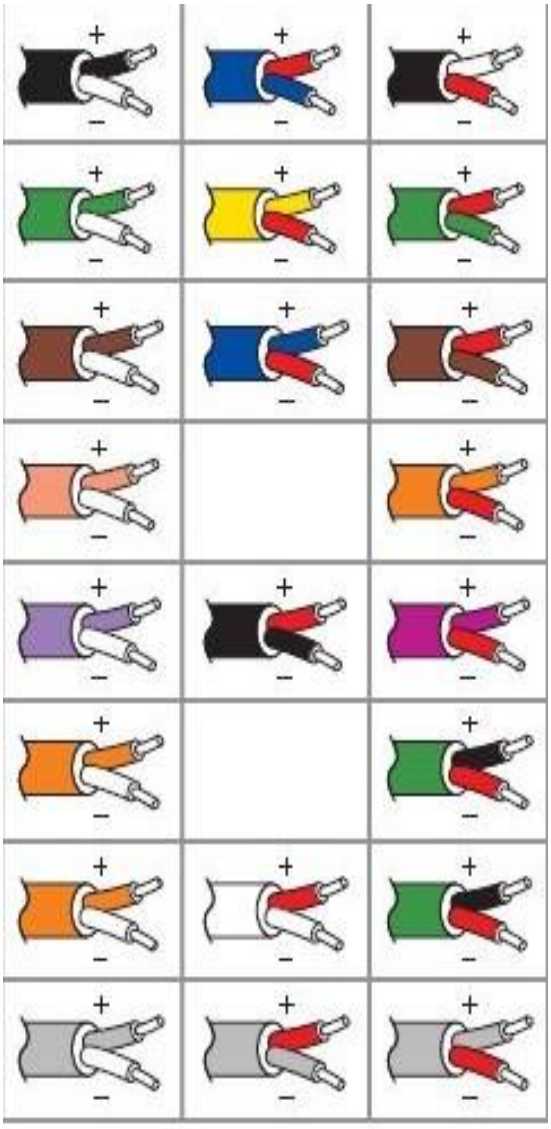		
K	Ni-Cr	Ni-Al	-270 to 1372			
T	Cu	Cu-Ni	-270 to 400			
N	Ni-Cr-Si	Ni-Cr-Mg	-270 to1300			
E	Ni-Cr	Cu-Ni	-270 to 1000			
R	Pt-%13 Rh	Pt	-50 to 1768			
S	Pt-%10 Rh	Pt	-50 to 1768			
B	Pt-%30 Rh	Pt- %6 Rh	0 to 1720			

3. THERMOCOUPLE CALIBRATION

The fixed-point method commonly used in high precision calibrations involves the use of phase change temperatures of substances such as water, zinc or argon [2]. Thus, it correlates the temperature readings provided by the measuring tool with fixed values of the phase change temperatures of the substance used. As a result, it is possible to determine a characteristic equation from the measuring tool via linear regression. It should be noted here that the use of this equation is recommended only for the range bounded by the phase change points of the specified substance.

In this experiment, K-type thermocouple calibration has been performed using the fixed-point method and distilled water. With the use of pure water, possible temperature differences during phase change are eliminated. Two temperatures are taken into account as reference points. These are the ice-water mixture temperature (0 °C) and the boiling temperature of water (97.429 °C), which corresponds to the measured pressure of our laboratory environment (92.77 kPa). It is known that there is a difference between the temperature value measured by thermocouples and the actual value. For this reason, the actual temperature values corresponding to the temperature values read from the thermocouples were found within the scope of this experiment with the equations obtained from the linear regression curve.

4. PROCEDURE OF THE EXPERIMENT

1. The ends of the thermocouples are soldered.
2. The other open ends of the thermocouples are connected to the data logger tape.
3. With the positive lead to the positive socket, the negative lead to the negative socket.
4. The tape is inserted into the data logger.
5. Thermocouples are immersed in boiling water and temperatures are recorded with the data logger.
6. Thermocouples are immersed in ice-water and temperatures are recorded with the data logger.

5. OBTAINING THE CALIBRATION CURVE

It is possible to remove the difference between the actual temperature value and the temperature values read from the thermocouple, by creating a calibration curve for each thermocouple. Thus,

a linear equation of each thermocouple can be obtained and the actual temperature values of the thermocouples can be read.

Example:

When the K type thermocouple is immersed in ice water at 0 °C, the reading temperature from thermocouple is 0,531 °C. When the same thermocouple was immersed in boiling water at 97,429 °C, the reading temperature from thermocouple is 97,275 °C.

Table 2. Temperature values

Reference Temperature (°C)	Thermocouple temperature (°C)
0	0,531
97,429196	97,275

Figure 3 shows the linear calibration curve obtained from the temperature values. The linear equation between the reference temperature and the reading temperature from the thermocouple is given above the curve. Now the actual value corresponding to the value measured by the thermocouple can be determined.

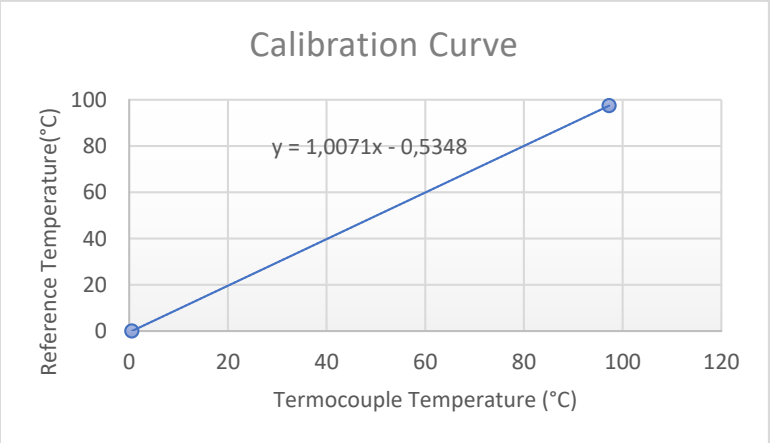

Figure 3. Calibration curve

7. EXPERIMENT REPORT

1. Write and explain the thermocouple calibration methods.

2. In the table below, the reading temperature from the thermocouple and the reference temperatures in the experiment are given. Derive the calibration curve and equation for these temperatures using Microsoft Excel. Fill in the blanks in the table. (T_r: Reference temperature, T_t: reading temperature from thermocouple, T_k: Temperature obtained from the calibration equation, E: Percentage of error between the temperature obtained from the calibration equation and the reference temperature)

	T_g (°C)	T_t (°C)	T_k (°C)	Equation	E (%)
1	0	0,66			
	97,429196	98,024			
2	0	0,504			
	97,429196	98,045			
3	0	1,234			
	97,429196	97,371			

REFERENCES

[1] Allred, D. D., "SCT-93 short course on thermoelectrics: An overview of thermoelectricity'', Technical Report, The International Thermoelectric Society, (1993).
[2] J.V. Pearce, V. Montag, D. Lowe, W. Dong, Int. J. Thermophys. (2011). https ://doi.org/10.1007/s1076 5-010-0892-8

EXPERIMENT 3

INVESTIGATION OF THE EFFECT OF CUTTING SPEED ON SURFACE ROUGHNESS

1.AIM

The purpose of this experiment is to determine the surface roughness of machined parts and to examine the effect of cutting speed from on the surface roughness.

2.THEORY

Depending on the processing method, the type of cutter and the material being processed, undesired scratches form on the machined surfaces due to physical, chemical, thermal factors and physical contact between cutter and the surface being cut. These irregular deviations below and above the nominal surface line, is called surface roughness.

The quality of treated surfaces plays an important role in machining performance. The quality of machined surfaces significantly improves fatigue strength, corrosion resistance and friction. Surface roughness also affects various functional properties of parts such as surface friction-causing contact, wear, heat conduction, ability to hold and distribute oil film, coating or resistance life. For this reason, the desired surface finish is usually determined beforehand and appropriate processes are selected to achieve the quality needed.

Surface roughness in machining is affected by the following factors:

- Rigidity of machine tool,
- Errors caused by bearing system,
- Tool holder rigidity,
- Effects of tool wear,
- Tool geometry,
- Cutting parameters,
- Mechanical properties of the material,
- Effects of coolant.

Factors like cutting speed, feed and chip length are controllable parameters of the operation. However, tool geometry, tool wear, chip loads and chip formations or material properties of tool and workpiece are uncontrollable parameters.

Machine tool vibration, irregularities in the workpiece, tool wear, or irregularities of the chip formation cause the surface to deteriorate during machining.

Estimating surface roughness and assessing the machining parameters such as feed rate or cutting speed improves product quality and ensures the desired surface roughness is achieved.

In machining, better surface quality is usually achieved at high cutting speeds. But the same surface quality can't be maintained for a long time as high cutting speeds accelerates tool wear.

The relationship of the average ideal surface roughness obtained in the machining operation with a single-rim cutting tool with the tool tip radius and feed rate is shown in the following equation:

$$R_i = \frac{f^2}{32r}$$

R_i : Ideal average surface roughness,mm

f : Feed rate, mm/dev

r : Tool tip radius,mm

The actual surface formed becomes rougher than the ideal surface due to the parameters affecting the surface roughness. By taking these parameters into account, a correction factor can be developed between ideal and true surface roughness. The correction factor between the real surface roughness and ideal surface roughness is shown in Figure 1. Depending on the ideal surface roughness, the actual surface roughness is expressed by the following equation:

$R_a = r_{ai} R_i$

R_a : True surface roughness

r_{ai} : Correction factor

R_i : Ideal surface roughness

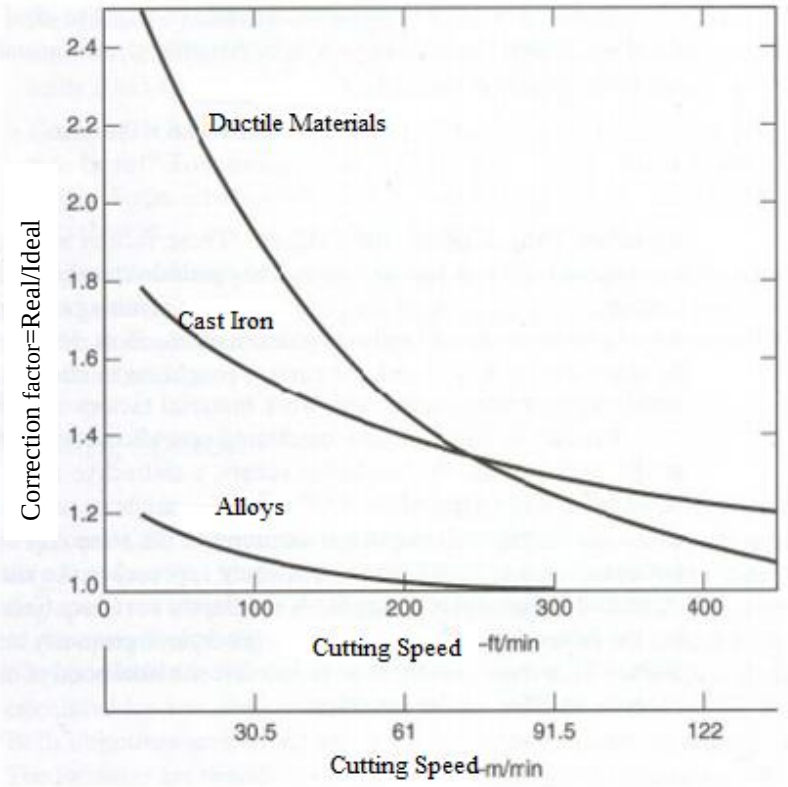

Figure 1. Surface roughness correction factor

Surface Roughness Measurement

In the experiment, the pits and peaks formed on the surface will be measured with the help of a Taylor Hubson 3+ Surface Roughness Measurement Device (Figure 2).

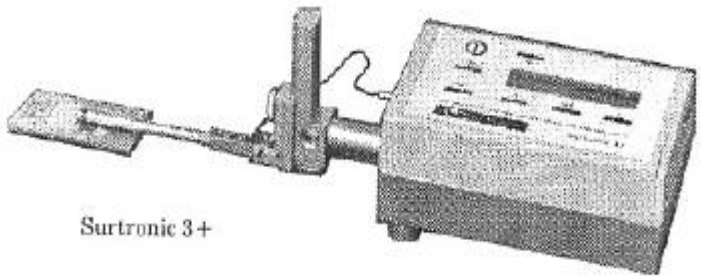

Figure 2. Taylor Hubson 3+ Surface Roughness Measurement Device

While calculating the roughness of a surface profile, the reference line, which evenly cuts the areas above and below the surface and is called the mean line, is used (Figure 3). This line can also be expressed mathematically in the form of the center of gravity of the surface profile (L_c).

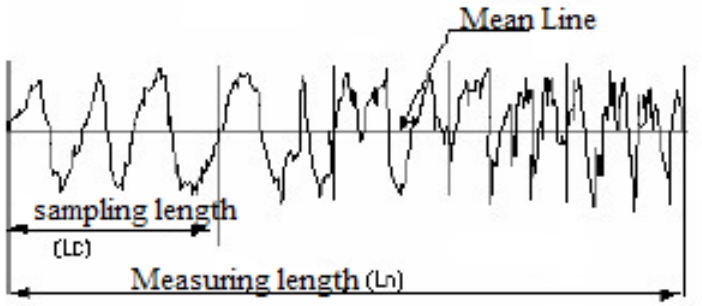

Figure 3. Measurement and sampling length

Sampling length is first parameter to be selected for finding the roughness characteristic of the surface. The measurement length L_n is formed by the combination n sampling length (Figure 3).

Average Surface Roughness (R_a) **:**

The mean surface roughness is the arithmetic mean of the changes in height measured from the mean line.

$$R_a = \frac{1}{l} \int_0^1 |Z\ (x)|\ dx$$

R_a values are calculated automatically by the device used in the experiment.

The symbols used to indicate surface roughness and characteristic are shown in Figure 4.

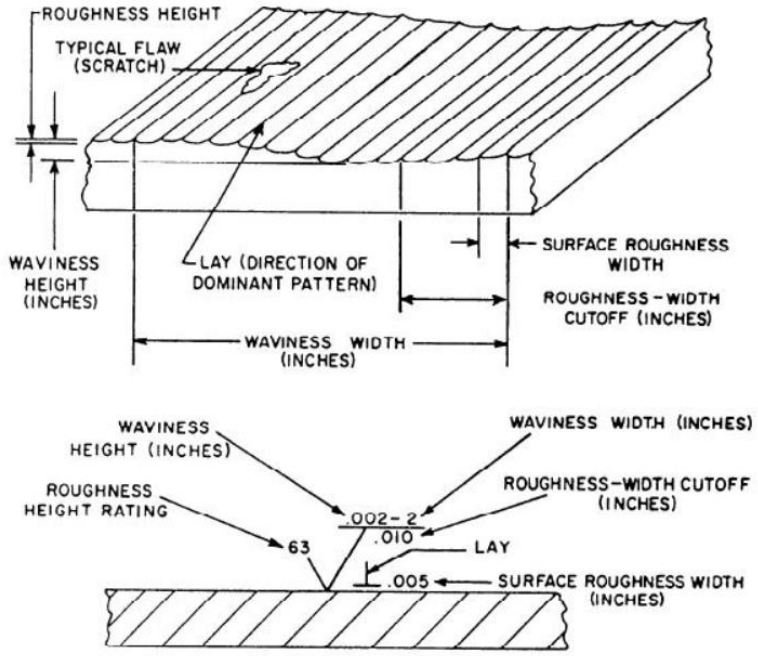

Figure 4. Surface characteristics and symbols

3. DEVICE AND EQUIPMENT

The lathe will be used in this experiment is located in the Machine Tools Laboratory of the Mechanical Engineering Department.

4. METHOD

1. Ç1010, Ç1020 or Ç1030 round material is provided for turning.
2. A hard metal cutting tool with a 0.4 radius is selected and is not changed throughout the experiment.
3. The workpiece is mounted to the fixture and the surface is machined with 30 mm increments at changing cutting speeds 20, 40, 80 and 140 m/min. (Figure 5).

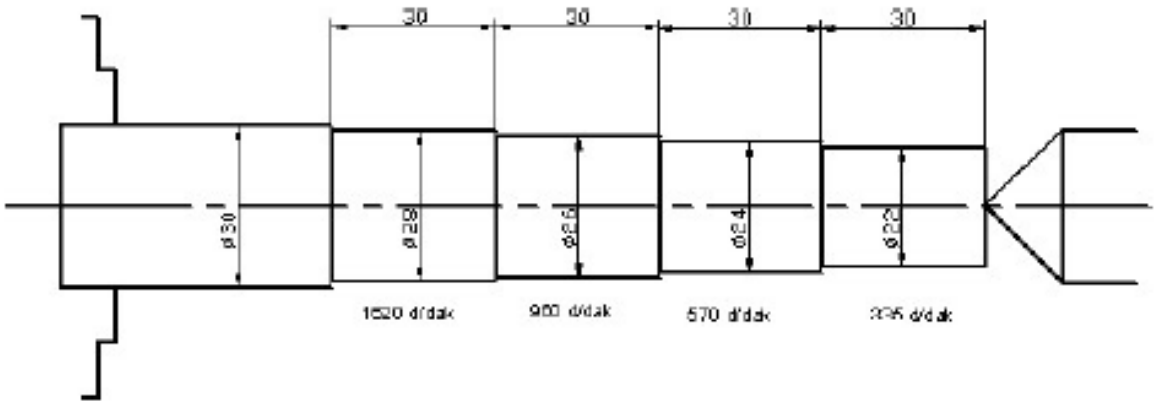

Figure 5. Machined workpiece

4. At least 3 measurements of each diameter are taken with the surface roughness measuring device.

5. The surface roughness of the parts is calculated.

5. REPORT AND EVALUATION

Machined parts on the lathe:

1. Since the machined diameters are different, even if they are smaller than the given measurements, calculating the actual value of each diameter and the cutting speed values obtained by utilizing the machine's working speed.
2. Comparison and interpretation of the surface roughness values measured with the surface roughness device and those obtained from calculations.
3. Comparison and interpretation of the cutting speed parameter that affects surface roughness.

6. RESOURCES

1. Akkurt, M., "Makina Elemanları Cilt II", Birsen Yayınevi, İstanbul (2000).
2. Akkurt, M., ''Talaş Kaldırma Yöntemleri ve Takım Tezgahları'', Birsen Yayınevi, İstanbul (1998).
3. Güllü, A., "Silindirik Taşlamada İstenen Yüzey Pürüzlüğünü Elde Etmek İçin Taşlama Parametrelerinin Bilgisayar Yardımıyla Optimizasyonu", Doktora Tezi, Gazi Üniversitesi Makine Eğitim Bölümü, Ankara, (1995).
4. Huynh, V., M., Fan, Y., "Surface-Texture Measurement and Characterization with Applications To Machine-Tool Monitoring". The International Journal of Advanced Manufacturing Technology, 7, 2-10,(1992).
5. Jang, D.Y., Choi, Y.G., Kim, H.G., Hsiao, A., "Study of The Corelation Between Surface Roughness and Cutting Vibrations To Develop An Online Roughness Measuring Tecnique_n Hard Turning", International Journal of Machine Tools Manufacture, 36(4), 453-464(1996).
6. Özses, B., ''Bilgisayar Sayısal Denetimli Takım Tezgahlarında Değişik İşleme Koşullarının Yüzey Pürüzlülüğüne Etkisi''. Yüksek Lisans Tezi, Gazi Üniversitesi Fen Bilimleri Enstitüsü, Makine Mühendisliği Bölümü, Ankara, (2002).
7. Onwubolu, G., C., "Surface Roughness Prediction Model in Machining of Carbon Steel by PVD Coated Cutting Tools" American Journal of Applied Sciences, 2 (6), 1109-1112 (2005).
8. Groover, M., P., "Fundamentals of Modern Manufacturing- Materials, Processes and Systems", Prentice-Hall Inc., New Jersey, 220-639(1996).

EXPERIMENT 4
MODULUS OF ELASTICITY AND RIGIDITY DETERMINATION IN MATERIALS WITH BENDING AND TORSION TESTS

1. OBJECTİVE

The aim of the bending test is to examine the relation between the load, beam thickness, beam width and beam length and deflection applied with a beam in a beam and obtaining the elasticity module of the steel material.

In the torsion test, the aim is to find shear modules of steel, brass and aluminum samples by examining the change of torsion angle with torsional moment and shaft length in a shaft.

2. THEORY

2.1 Bending Test

Elements supported by one or more points and loaded perpendicular to the rod axis are called beams. Beams are subject to bending load. As a result of the bending test, besides general information about the deformation properties of the materials, values such as bending moment, bending stress, modulus of elasticity and bending amount (deflection) are calculated. The elasticity module can be determined by the tensile test or bending test.

In this experiment, the elasticity module of the material will be calculated without exceeding the elastic region by applying stresses less than the yielding point of the material.

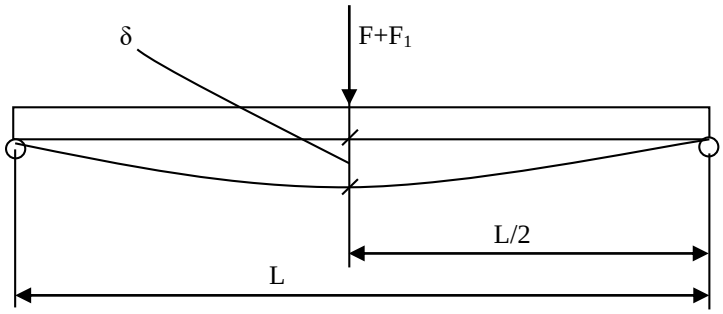

Şekil 1. Bending Test

Deflection formula for simple supported beam (Fig. 1), where the force F is applied from its midpoint:

$$\delta = \frac{FL^3}{48EI} \quad (1)$$

The bending stress σ_b is

$$\sigma_b = \frac{M_b c}{I} \quad (2)$$

Where

δ = Deflection (mm)

L = Beam length (mm)

M_b = Bending Moment (Nmm)

σ_b = Bending Stress (N/mm^2)

E = Elasticity Module (N/mm^2)

I = The moment of Inertia (mm^4)

F_1 = the weight of load arm (N)

F = Added weight (N)

C = h/2 (mm)

For rectangular section $I = \frac{bh^3}{12}$, and circular section $I = \frac{\pi d^4}{64}$.

2.2 Torsion Test

Torsion test is generally done to determine the properties of materials such as shear elasticity modulus and shear yield stress. In the torsion test, a shaft is fixed at one end and the torsion angle and torsional moment are recorded by rotating the free end. The torsion moment-torsion angle curve, called the torsion diagram, is drawn from the values obtained.

The samples with a circular cross section (shafts) are subject to torsion stress. Shear stresses occur in the sample due to the torsional moment applied during the experiment. These stresses increase linearly from the center of the sample to the surface. The shear stress is maximum at the surface of the sample while it is zero in the center of the sample.

Shear stress on the surface of the circular cross-section sample in the torsion test is

$$\tau = \frac{Tr}{J} \qquad (3)$$

If the J, polar moment of inertia in the Eqn. (3) is replaced

$$\tau = \frac{16T}{\pi d^3} \qquad (4)$$

General formula of torsional angle is

$$\phi = \int_0^L \frac{T(x)dx}{J(x)G} \qquad (5)$$

If expression (5) is integrated for constant torsional moment and constant cross section

$$\phi = \frac{TL}{JG} \qquad (6)$$

Where ϕ is radians.

3. EXPERIMENTAL TOOLS AND DEVICES

3.1. Test Device

Torsion and Flexural Tester MT 210 will be used as test setup.

3.2. Test Samples

The beams are made of 650 mm long steel material. The distance between each line in the beam is 100 mm. Beam sections are as follows: 3x25 mm, 4x25 mm, 6x25 mm, 8x25 mm, 4x15 mm, 4x20 mm and 4x30 mm.

The samples used in the torsion test are made of 8 mm diameter steel, aluminum and brass materials and they are 650 mm long. As in beams, the distance between each line is 100 mm. The weight of the arm on which the weights will be hung is 2.5 N. In addition, there are 4 weights of 5 N each. A dial gauge with an accuracy of 0.01 mm will be used as a measuring instrument.

4. EXPERIMENTAL STUDIES

4.1. Implementation of Bending Experiment

- **Examining the Relationship Between Load and Deflection:**

Bearings are placed on both ends of the 600 mm beam. Between the two lines marked on the beam is 100 mm. The test sample with a section length of 6x25 mm is placed in the supports. The weight assembly is hung right in the center of the test sample. A measuring instrument is placed on the top surface of the weight assembly and reset. Thus, the test setup is installed. Then the weights are put one by one and the amount of deflection is measured.

- **Examining the Relationship Between Beam Length and Deflection:**

The load is kept constant at 10 N and deflections at different support distances (300 mm, 400 mm, 500 mm, 600 mm) of the test specimen of 6x25 mm are measured.

- **Examining the Relationship Between Beam Width and Deflection:**

The deflections in different widths (15 mm, 20 mm, 25 mm, 30 mm) are measured by taking the beam length 600 mm, the beam thickness 4 mm and the load 5 N.

- **Examining of Correlation Between Beam Thickness and Deflection:**

The deflections in different thickness (3 mm, 4 mm, 6 mm, 8 mm) beams are measured by taking the beam length 600 mm, beam width 25 mm, and the load 5 N.

Note: When calculating Elasticity Module E, the gauge should be reset for deflection caused by the first weight (weight arm). However, when calculating bending stress, the first weight should be taken into account.

Implementation of Torsion Testing

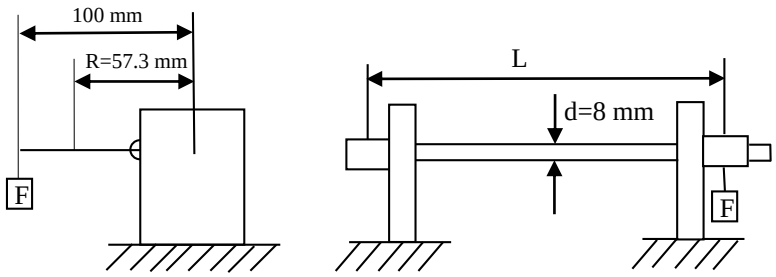

Şekil 2. Torsion Test Mechanism

- **Finding the Relationship between Torsion Moment and Torsion Angle:**

One end of the test sample is fixed and the other is released. Sample length is adjusted to 600 mm. A gauge is placed in the notch on the free end of the arm and then reset. The notch on the torsion arm and the shaft axis are set at 57.3 mm. At this distance, the deviation of 1mm in the measuring instrument corresponds to 1 degree. Torsion angles are found by applying loads of 2.5 N, 7.5 N, 12.5 N and 17.5 N at a distance of 100 mm from the axis of the circular cross section bar.

- **Finding the Relationship Between Sample Length and Torsional Angle:**

Torsion angles are found by keeping the load constant at 12.5 N and adjusting the sample lengths to 300 mm, 400 mm, 500 mm and 600 mm.

5. CALCULATIONS AND REQUESTED

- Draw the diagram showing the deflection as a function of the load.
- Draw the diagram showing the deflection as a function of the beam length.
- Draw the diagram showing the deflection as a function of the beam width.
- Draw the diagram showing the deflection as a function of the beam thickness.
- For each load, calculate the bending moment, bending stress, deflection, and elasticity modulus, and present the results in a table. Then, calculate the average elasticity modulus.
- For each load, calculate the torsion moment, torsion angle, torsional shear stress, and shear elasticity modulus, and present the results in a table. Then, calculate the average shear elasticity modulus.
- Draw a diagram showing the torsion angle as a function of the torsion moment.
- For each sample length, calculate the torsion angle and draw a diagram showing the torsion angle as a function of the sample length.
- Compare the theoretical and experimental results.
- Perform an error analysis.
- Explain the reasons for the errors.

EXPERIMENT 5

FORCED VIBRATION OF AN UNDAMPED ONE-DEGREE-OF-FREEDOM SYSTEM DUE TO HARMONIC EXCITATION

1 INTRODUCTION

Vibrations of mechanical systems can be classified into two categories: free vibrations and forced vibrations. Free vibrations are oscillations around a system's equilibrium position that occur in the absence of an external excitation. If any kind of external force acts on a system during vibration, the vibration of the system is called forced vibration. In this experiment, the forced vibration of a rectangular beam with harmonic excitation will be examined and experimental results will be compared with the analytical solution of the equation of motion.

2 THEORY

2.1 Free Vibrations of One-Degree-of-Freedom Undamped Systems

Any single freedom undamped mechanical system can be represented by equivalent systems model illustrated in Figure 2.1. If the generalized coordinate is selected to be a displacement, then the system can be represented with an equivalent mass and equivalent stiffness. Similarly, the system can be represented with an equivalent inertia and equivalent torsional stiffness for angular generalized coordinates. The equation of motion for these systems can be obtained by applying Newton's second law of motion as such:

$$m_{eq}\ddot{x} + k_{eq}x = 0 \qquad \textbf{2.1}$$

$$I_{eq}\ddot{\theta} + k_{t_{eq}}\theta = 0 \qquad \textbf{2.2}$$

Equation 2.1 and 2.2 are second order linear homogeneous differential equations. For a more detailed explanation on the subject of ordinary differential equations you can refer to an elementary differential equation textbook [2]. The solutions of these homogeneous differential equations are:

$$x_h(t) = C_1 \cos\left(\sqrt{\frac{k_{eq}}{m_{eq}}}\,t\right) + C_2 \sin\left(\sqrt{\frac{k_{eq}}{m_{eq}}}\,t\right) \qquad \textbf{2.3}$$

$$\theta_h(t) = C_1 \cos\left(\sqrt{\frac{k_{t_{eq}}}{I_{eq}}}\,t\right) + C_2 \sin\left(\sqrt{\frac{k_{t_{eq}}}{I_{eq}}}\,t\right) \qquad \textbf{2.4}$$

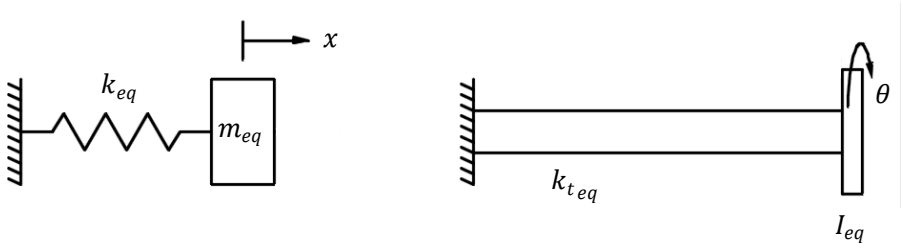

Figure 2.1: Equivalent systems model of a linear one-degree-of-freedom undamped system with a linear displacement as generalized coordinate(on the left), with an angular coordinate(on the right)

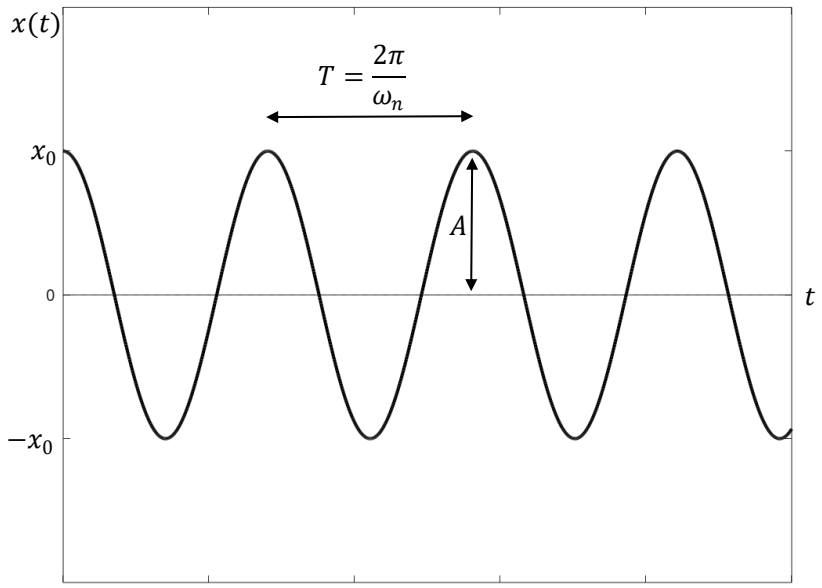

Figure 2.2: Free vibration response of an undamped system

It can be observed from Equation 2.3 and 2.4 that the two systems vibrate around the equilibrium positions at frequencies $\sqrt{\frac{k_{eq}}{m_{eq}}}$ and $\sqrt{\frac{k_{t_{eq}}}{I_{eq}}}$. These two frequencies are referred as natural frequencies and often represented with ω_n in the literature. They represent the oscillation characteristics of mechanical systems in the absence of an external excitation. Figure 2.2 illustrates the solution of Equation 2.3 with initial conditions $x(0) = x_0$, and $\dot{x}(0) = 0$. Since the system does not have any damping member, the system is to be expected to oscillate around the equilibrium point continuously without losing its energy.

2.2 Free Vibrations of One-Degree-of-Freedom Damped Systems

Similar to the undamped systems, damped systems can also be modeled using equivalent systems. However, this time an equivalent damping member must be included in the system. In mechanical systems, damping occurs due to dry friction and viscous friction. Figure 2.3 shows equivalent system models and the equations of motion can be obtained as follows:

$$m_{eq}\ddot{x} + c_{eq}\dot{x} + k_{eq}x = 0 \quad \textbf{2.5}$$

$$I_{eq}\ddot{\theta} + c_{t_{eq}}\dot{\theta} + k_{t_{eq}}\theta = 0 \quad \textbf{2.6}$$

At this point it would be useful to express Equation 2.5 and 2.6 in a simplified form:

$$\ddot{x} + 2\zeta_x\omega_{n_x}\dot{x} + \omega_{n_x}^2 x = 0 \quad \textbf{2.7}$$

$$\zeta_x = \frac{1}{2}\frac{c_{eq}}{\sqrt{k_{eq}m_{eq}}}, \qquad \omega_{n_x} = \sqrt{\frac{k_{eq}}{m_{eq}}} \quad \textbf{2.8}$$

$$\ddot{\theta} + 2\zeta_\theta\omega_{n_\theta}\dot{\theta} + \omega_{n_\theta}\theta = 0 \quad \textbf{2.9}$$

$$\zeta_\theta = \frac{1}{2}\frac{c_{t_{eq}}}{\sqrt{k_{t_{eq}}I_{eq}}}, \qquad \omega_{n_\theta} = \sqrt{\frac{k_{t_{eq}}}{I_{eq}}} \quad \textbf{2.10}$$

New parameters(ζ_x, ζ_θ) appearing in Equation 2.7 and 2.9 are called damping ratios. The simplified form serves two main purposes: first is to nondimensionalize the equivalent damping in the system and second is to present the solution in a compact form. The solution of these equations in the simplified form is given for $\zeta_x < 1$ and $\zeta_\theta < 1$ as:

$$x_h(t) = e^{-\zeta_x\omega_{n_x}t}\left[C_1\cos\left(\omega_{n_x}\sqrt{1-\zeta_x^2}t\right) + C_2\sin\left(\omega_{n_x}\sqrt{1-\zeta_x^2}t\right)\right] \quad \textbf{2.11}$$

$$\theta_h(t) = e^{-\zeta_\theta\omega_{n\theta}t}\left[C_1\cos\left(\omega_{n\theta}\sqrt{1-\zeta_\theta^2}t\right) + C_2\sin\left(\omega_{n\theta}\sqrt{1-\zeta_\theta^2}t\right)\right] \quad \textbf{2.12}$$

Unlike undamped systems, the system is expected to produce decaying oscillations around the equilibrium point in free vibrating and damped systems. The vibration characteristic of this type of systems are illustrated in Figure 2.4 by giving solution to Equation 2.11 with initial conditions $x(0) = x_0$, and $\dot{x}(0) = 0$.

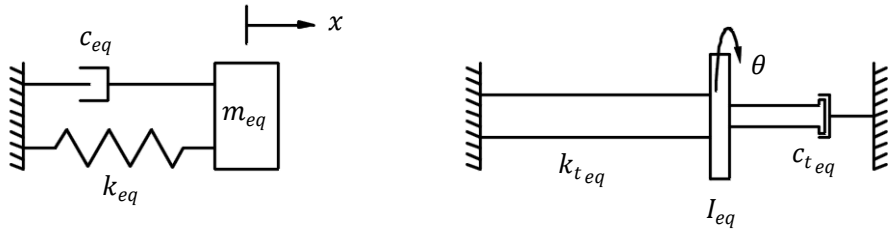

Figure 2.3: Equivalent systems model of a linear one-degree-of-freedom damped system

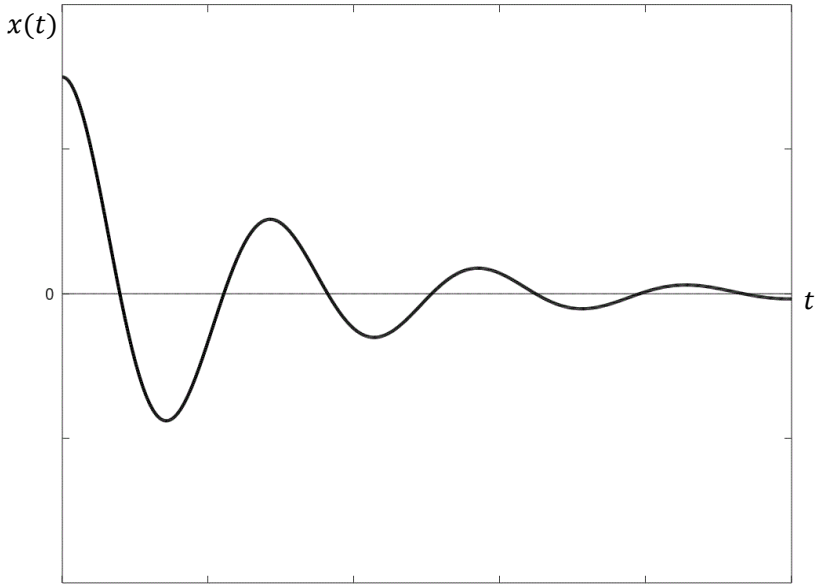

Figure 2.4: Free vibration response of a damped system

2.3 Forced Vibrations of One-Degree-of-Freedom Undamped Systems

As explained in the previous section, if a system is subjected to an external excitation the vibration of the system is called forced vibrations. The equivalent system models of such systems are given in Figure 2.5. Using equivalent system models it is possible to obtain the equations of motion for these systems:

$$\ddot{x} + \omega_{n_x}^2 x = \frac{1}{m_{eq}} F_{eq}(t) \qquad \textbf{2.13}$$

$$\ddot{\theta} + \omega_{n_\theta} \theta = \frac{1}{I_{eq}} M_{eq}(t) \qquad \textbf{2.14}$$

We are only interested harmonic type excitations in this experiment. An excitation is periodic(harmonic) if there exists a time period T for all t such that:

$$F_{eq}(t + T) = F_{eq}(t) \qquad \textbf{2.15}$$

Also, the frequency of a harmonic excitation is defined as:

$$\omega = \frac{2\pi}{T} \qquad \textbf{2.16}$$

In this experiment we will be dealing with a single-frequency excitation which has the following form:

$$F_{eq}(t) = F_0 \sin(\omega t + \psi) \quad \textbf{2.17}$$

where F_0 is the amplitude of the excitation, ω is its frequency, and ψ is its phase. It should be noted that the excitation frequency is independent of the systems natural frequency.

The differential equations given in Equation 2.13 and 2.14 are no longer homogeneous due to equivalent force and moment terms on the right hand side. The general solution of nonhomogeneous differential equations can be obtained as follows:

$$x_g(t) = x_h(t) + x_p(t) \quad \textbf{2.18}$$

where $x_h(t)$ is homogeneous part of the solution which was obtained in Equation 2.3 and $x_p(t)$ represents the particular solution and it depends on the form of $F_{eq}(t)$. Assuming $F_{eq}(t)$ has the form given in Equation 2.17 and with the initial conditions $x(0) = x_0$, and $\dot{x}(0) = \dot{x}_0$, the general solution of Equation 2.13 is obtained for the case $\omega \neq \omega_n$:

$$x_h(t) = C_1 \cos(\omega_n t) + C_2 \sin(\omega_n t) \quad \textbf{2.19}$$

$$x_p(t) = \frac{F_0}{m_{eq}(\omega_n^2 - \omega^2)} \sin(\omega t + \psi) \quad \textbf{2.20}$$

$$x_g(t) = \left[x_0 - \frac{F_0 \sin\psi}{m_{eq}(\omega_n^2 - \omega^2)}\right] \cos(\omega_n t) + \frac{1}{\omega_n}\left[\dot{x}_0 - \frac{F_0 \omega \cos\psi}{m_{eq}(\omega_n^2 - \omega^2)}\right] \sin(\omega_n t) + \frac{F_0}{m_{eq}(\omega_n^2 - \omega^2)} \sin(\omega t + \psi) \quad \textbf{2.21}$$

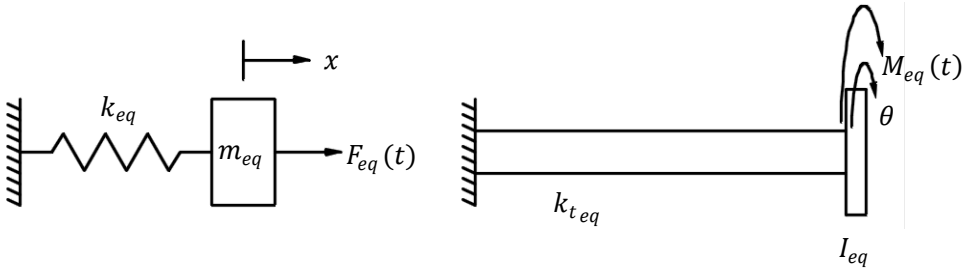

Figure 2.5: Equivalent systems model of a linear one-degree-of-freedom undamped system under external excitation

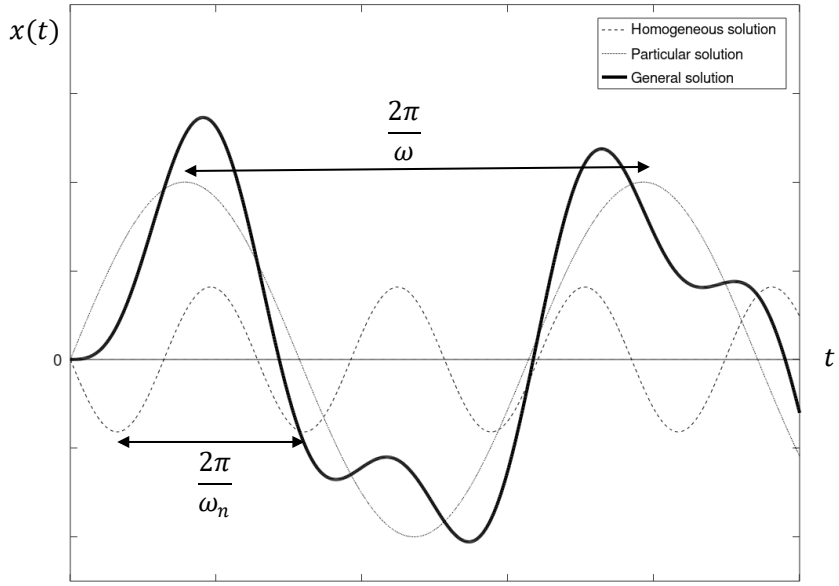

Figure 2.6: Forced vibration response of an undamped system under harmonic excitation

The system response plotted in Figure 2.6 is the sum of two trigonometric functions with different frequencies. The case $\omega = \omega_n$ is special and when excitation frequency equals natural frequency the homogeneous and particular solutions becomes linearly dependent. Therefore, another particular solution is needed for this case. If $F_{eq}(t)$ has the form given in Equation 2.22, the particular and general solutions are given as:

$$F_{eq}(t) = F_0 \sin(\omega_n t + \psi) \qquad \textbf{2.22}$$

$$x_p(t) = -\frac{F_0}{2m_{eq}\omega_n} t \cos(\omega_n t + \psi) \qquad \textbf{2.23}$$

$$x_g(t) = x_0 \cos(\omega_n t) + \left(\frac{\dot{x}_0}{\omega_n} + \frac{F_0 \cos\psi}{2m_{eq}\omega_n^2}\right) \sin(\omega_n t) - \frac{F_0}{2m_{eq}\omega_n} t \cos(\omega_n t + \psi) \qquad \textbf{2.24}$$

The response of a system in which the excitation frequency equals the natural frequency grows without bounds as illustrated in Figure 2.7. This condition where amplitude increases without bound, is called *resonance*. Although mathematically possible, in a real physical system vibration amplitudes are bounded and they cannot continuously grow due to damping effects present within the system. Resonance is a dangerous condition in a mechanical or structural system and will result in undesired large displacements or failure. Resonant torsional oscillations were partially the cause of famous Tacoma Narrows Bridge disaster [3]. Therefore, an engineer should always be aware of the natural resonant frequencies of the system to be designed and the working conditions.

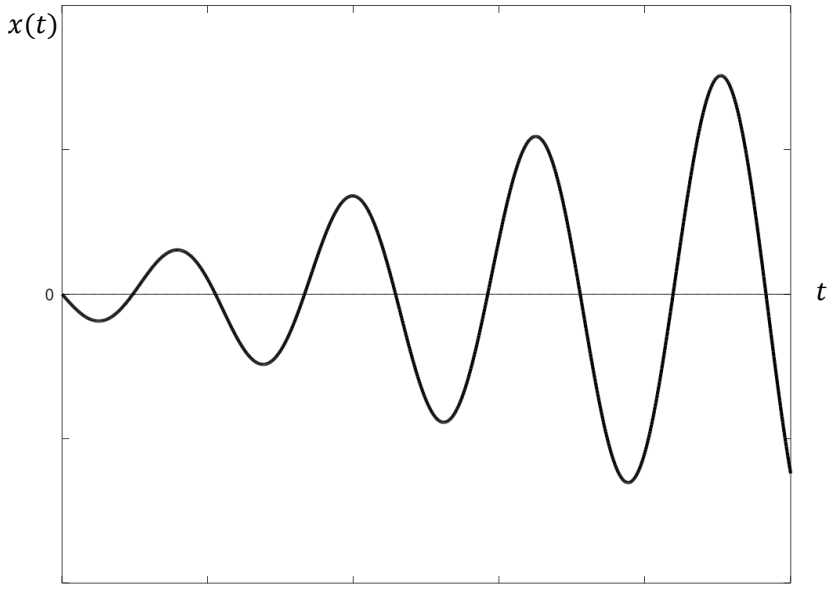

Figure 2.7: Undamped response when excitation frequency equals natural frequency. The response grows without bounds producing resonance.

2.4 Model of the Experimental Setup

The model given in Figure 2.8 consists of following parts.

i. Rigid AD beam with mass m and length L, connected to the ground with a revolute joint at point A.
ii. Spring with a stiffness k, connected to the beam at point C.
iii. Motor unit with mass M which rotates two unbalanced disks at constant angular speed of ω attached to the beam at point B. Each disk has unbalanced weights with mass m_u and eccentricity e.
iv. Detachable weights at point D with mass m_d (total number of n) which allows the equivalent mass of the system to be altered.

The equation of motion of the system can be obtained as follows:

$$\left(\frac{1}{3}mL^2 + ML_1^2 + nm_dL_2^2\right)\ddot{\theta} + kL_2^2\theta = m_u e L_1 \omega^2 \sin(\omega t) \qquad \textbf{2.25}$$

It would be more convenient to express Equation 2.24 in the simplified format:

$$\ddot{\theta} + \omega_n^2\theta = F_0 \sin(\omega t) \qquad \textbf{2.26}$$

$$\omega_n = \sqrt{\frac{k\,L_2^2}{\left(\frac{1}{3}mL^2 + ML_1^2 + nm_dL_2^2\right)}} \qquad \textbf{2.27}$$

$$F_0 = \frac{m_u e L_1 \omega^2}{\left(\frac{1}{3}mL^2 + ML_1^2 + nm_d L_2^2\right)} \qquad \textbf{2.28}$$

As mentioned earlier forced vibration response of an undamped system consists of two parts: a homogeneous and a particular solution. Although the system is modeled as undamped, in a real system there are small damping effects present like joint friction and air resistance. Therefore, as the system response approaches steady-state, the effect of the homogeneous solution disappears due to damping and particular solution dictates the motion of the system. This ultimately means, at the steady-state the system will oscillate at the excitation frequency.

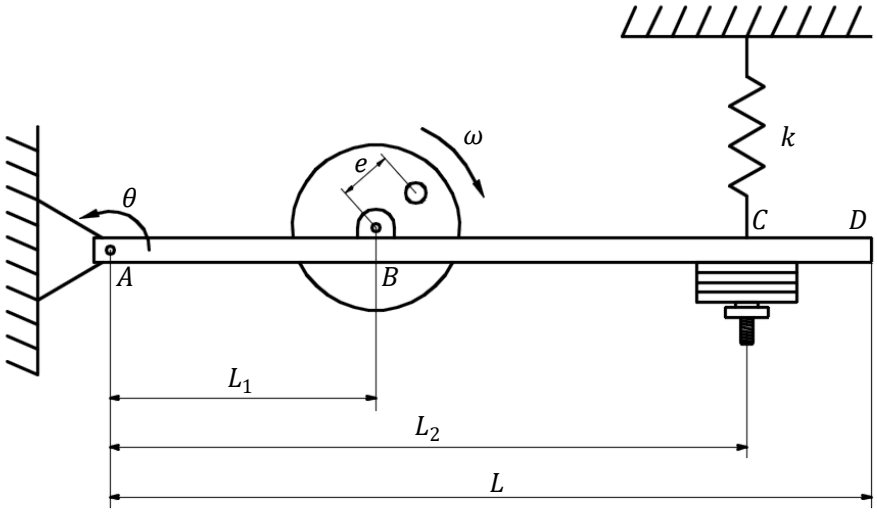

Figure 2.8: Model of the experimental setup

3 EXPERIMENTAL SETUP

The experimental setup given in Figure 3.1 consists of the following parts.

i. Rectangular beam: The beam is connected to the test bed with a revolute joint from one end and with a spring from the other. While the lower end of the spring is free to move, upper end is bolted to the test bed via a clamp. Using this clamp the relative position of the upper end of the spring can be adjusted.
ii. Motor unit: The motor unit is rigidly bolted to the beam. The harmonic excitation is obtained by rotating two unbalanced discs on the output shaft of the belt drive unit. The excitation frequency is adjusted by changing the rotational speed of the motor with the help of the speed control unit.
iii. Plotter: The vibration graph is obtained with a plotter fixed to the right end of the rectangular beam.

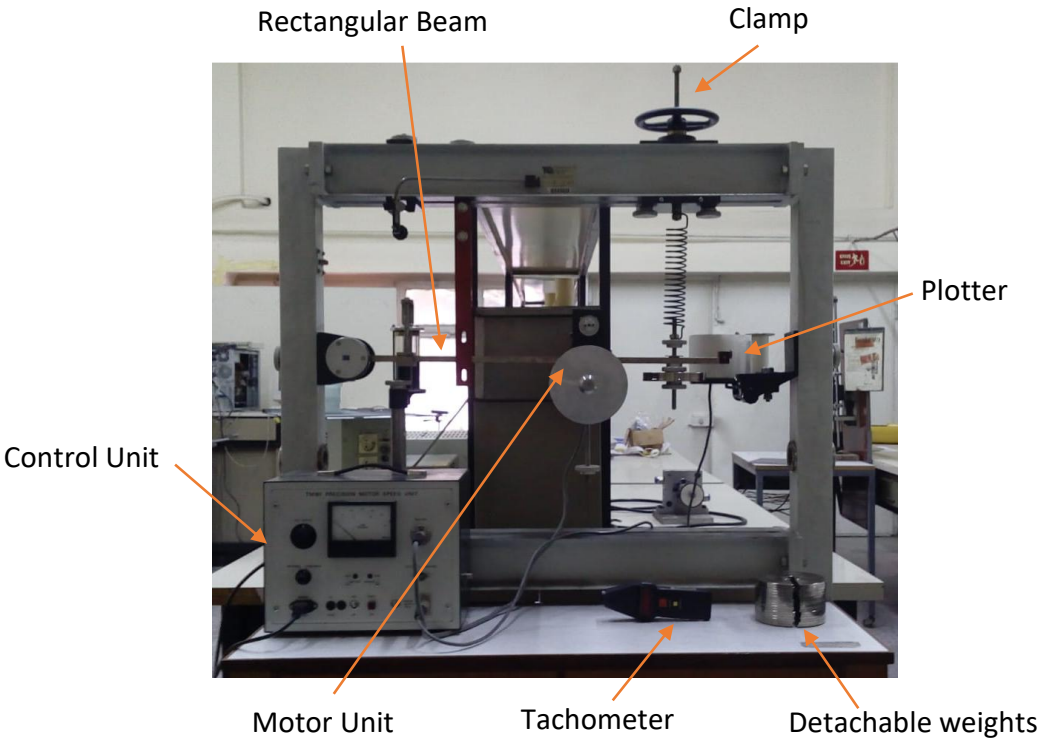

Figure 3.1: Experimental Setup

4 PROCEDURE OF EXPERİMENT

The electric cable of synchronous motor is plugged into the electric socket on the control unit. Then the beam is brought to the horizontal position by adjusting the clamp. The plotter position is adjusted so that the pencil located at the end of the beam lightly touches the paper roll. The numerical values of system parameters in the experiment are given in Table 3.1.

Table 3.1: Numerical values of the system parameters

Parameter	*Symbol*	*Value*	*Unit*
Motor unit mass	M	*4.930*	kg
Beam's mass	m	*1.922*	kg
Unbalanced mass	m_u	*33.051*	g
Mass of detachable weights	m_d	*400*	g
Eccentricity	e	*41.750*	mm

Before starting the experiment, measure the values of $L\ (m)$, $L_1\ (m)$, and $L_2\ (m)$. Also, take required measurements to calculate the spring constant $k\ (N/m)$.

During the experiment, measure the following for different values of the motor speed and try to determine the resonance frequency of the system.

i. Excitation Frequency: In this system, the excitation frequency is the angular speed of the motor. Measure the angular speed of the motor by counting the revolution of the disks at low speeds and using an optical tachometer at high speeds.
ii. Vibration Amplitude: Measure the amplitude of the vibration from the graph produced by the plotter on the beams right end.

5 REPORT

In the main part of your report followings should be included:

- Experimental data in tabular format,
- Calculations for the spring stiffness,
- The natural frequency of the system calculated using the analytical model,
- Frequency vs. amplitude curve to be plotted from the experimental data and resonant frequency of experimental setup determined from this graph.

In your conclusion, you are expected to comment on the followings:

- Does the natural frequency value calculated from the analytical model match the experimental results? Discuss possible causes of the difference between analytical and experimental results.
- According to the analytical model, the vibration amplitude of an undamped system must increase without bounds while it is in resonance. Discuss the factors that cause the resonance peak to be limited.

6 REFERENCES

1. Kelly, S. Graham. *Fundamentals of Mechanical Vibrations*. McGraw Hill, 2000.
2. Boyce, William E., et al. *Elementary Differential Equations and Boundary Value Problems*. Wiley, 2017.
3. *Tacoma Bridge - YouTube*. www.youtube.com/watch?v=3mclp9QmCGs.

EXPERIMENT 6
THE FORCED VORTEX EXPERIMENT

1. AIM

The aim of the experiment is to determine the pressure distribution in the fluid in a cylinder that performs forced vortex movement.

2. INTRODUCTION

If the fluid in a partially filled cylinder is rotated about its axis with a constant angular velocity ω, the relative velocities disappear in the cylinder after a short time and the liquid starts to act like a rigid body (Figure 1).

In a forced vortex, the velocity and pressure of the fluid increases due to energy supply from the outside. Centrifugal pumps operate with this principle. The liquid enters the pump at low pressure from the center. Its velocity and pressure increases as it travels from the center of the impeller to the outlet of impeller.

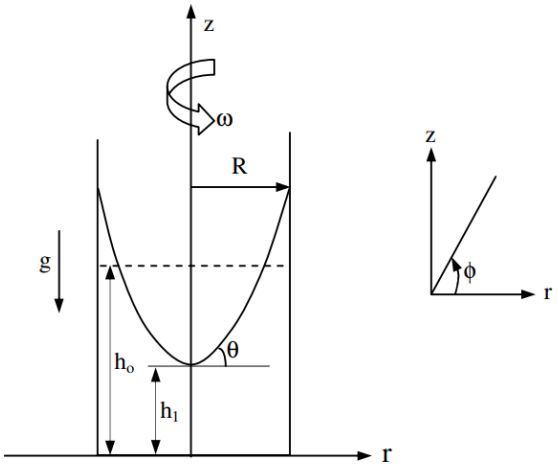

Figure 1. The surface and coordinate system of the fluid rotated with angular velocity ω

3. THEORY

Navier-Stokes equations in the cylindrical coordinate system written as

r direction:

$$\rho\left(\frac{\partial V_r}{\partial t}+V_r\frac{\partial V_r}{\partial r}+\frac{V_\phi}{r}\frac{\partial V_r}{\partial \phi}-\frac{V_\phi^2}{r}+V_z\frac{\partial V_r}{\partial z}\right)=F_r-\frac{\partial P}{\partial r}+\mu\left(\frac{\partial^2 V_r}{\partial r^2}+\frac{1}{r}\frac{\partial V_r}{\partial r}-\frac{V_r}{r^2}+\frac{1}{r^2}\frac{\partial^2 V_r}{\partial \phi^2}-\frac{2}{r^2}\frac{V_\phi}{\partial \phi}+\frac{\partial^2 V_r}{\partial z^2}\right) \quad (1)$$

ϕ direction:

$$\rho\left(\frac{\partial V_\phi}{\partial t}+V_r\frac{\partial V_\phi}{\partial r}+\frac{V_\phi}{r}\frac{\partial V_\phi}{\partial \phi}+\frac{V_r V_\phi}{r}+V_z\frac{\partial V_\phi}{\partial z}\right)=F_\phi-\frac{1}{r}\frac{\partial P}{\partial \phi}+\mu\left(\frac{\partial^2 V_\phi}{\partial r^2}+\frac{1}{r}\frac{\partial V_\phi}{\partial r}-\frac{V_\phi}{r^2}+\frac{1}{r^2}\frac{\partial^2 V_\phi}{\partial \phi^2}+\frac{2}{r^2}\frac{V_r}{\partial \phi}+\frac{\partial^2 V_\phi}{\partial z^2}\right) \quad (2)$$

z direction:

$$\rho\left(\frac{\partial V_z}{\partial t}+V_r\frac{\partial V_z}{\partial r}+\frac{V_\phi}{r}\frac{\partial V_z}{\partial \phi}+V_z\frac{\partial V_z}{\partial z}\right)=F_z-\frac{\partial P}{\partial z}+\mu\left(\frac{\partial^2 V_z}{\partial r^2}+\frac{1}{r}\frac{\partial V_z}{\partial r}+\frac{1}{r^2}\frac{\partial^2 V_z}{\partial \phi^2}+\frac{\partial^2 V_z}{\partial z^2}\right) \quad (3)$$

In forced vortex flow; the flow is steady, and $V_r, V_z, F_r, F_\phi, \frac{\partial V_\phi}{\partial \phi}$ values are zero. Considering these values, flow equations given above simplies significantly. Simplified equations are given below.

r direction:

$$\rho\left(-\frac{V_\phi^2}{r}\right)=-\frac{\partial P}{\partial r} \quad (4)$$

ϕ direction:

$$\frac{1}{r}\frac{\partial P}{\partial \phi}=0 \quad (5)$$

z direction:

$$\frac{\partial P}{\partial z}=-\rho g \quad (6)$$

Simplified equations show that pressure depends on radius and height of water column. ($P(r,z)$)

The forced vortex flow shown in Figure 2. The forced vortex flow, that is rigid body rotation, can be expressed as

$$V_\phi=\omega r\ . \quad (7)$$

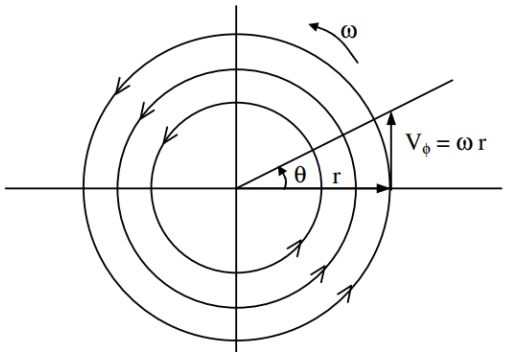

Figure 2. Streamlines in forced vortex

If we substitute the expression in (7) into the equation (4), the following pressure expression is obtained.

$$\frac{\partial P}{\partial r}=\rho\frac{(\omega r)^2}{r}=\rho\omega^2 r \quad (8)$$

By taking the integral of the above expression

$$P - P_1 = \rho\omega^2 \frac{\left(r^2 - r_1^2\right)}{2} + c(z) \tag{9}$$

The equation (9) is differentiated with respect to z and combined with equation (6)

$$\frac{\partial P}{\partial z} = -\rho g = c'(z)$$

If this equation is integrated

$$c(z) = -\rho g(z - z_1) \tag{10}$$

If Equation (10) is put in Equation (9),

$$P - P_1 = \rho\omega^2 \frac{\left(r^2 - r_1^2\right)}{2} - \rho g(z - z_1) \tag{11}$$

The point 1 is taken at central axis and fluid-air surface; $P_1=P_{atm}$, $r_1=0$, $z_1=h_1$. The equation (11) becomes as

$$P - P_{atm} = \rho\frac{\omega^2 r^2}{2} - \rho g(z - h_1) \tag{12}$$

If it is assumed that the pressure on the liquid surface is constant and equal to atmospheric pressure (P = Patm);

$$0 = \rho\frac{\omega^2 r^2}{2} - \rho g(z - h_1) \tag{13}$$

This equation can be arranged as free fluid surface to air

$$z = h_1 + \frac{\omega^2 r^2}{2g} \tag{14}$$

During forced vortex experiment, the volume of the water is constant, h_1 can be expressed as h_0 and R.

The volume of water without rotation:

$$V = \pi R^2 h_0 \tag{15}$$

The volume of water with rotation:

$$V = \int_0^R \int_0^z 2\pi r\,dz\,dr = \int_0^R 2\pi r z\,dr \tag{16}$$

$$V = \int_0^R 2\pi r\left(h_1 + \frac{\omega^2 r^2}{2g}\right)dr \tag{17}$$

The result is obtained;

$$V = \pi\left(h_1 R^2 + \frac{\omega^2 R^4}{4g}\right) \tag{18}$$

The constant volume of water results in equation (18).

$$h_1 = h_0 - \frac{(\omega r)^2}{4g} \tag{19}$$

Finally free surface height can be calculated as

$$z = h_0 - \frac{(\omega R)^2}{2g}\left(\frac{1}{2} - \left(\frac{r}{R}\right)^2\right) \tag{20}$$

4. TECHNICAL DATA

Pressure measurement points of forced vortex generated are given in Figure 3, the coordinates are given Table 1.

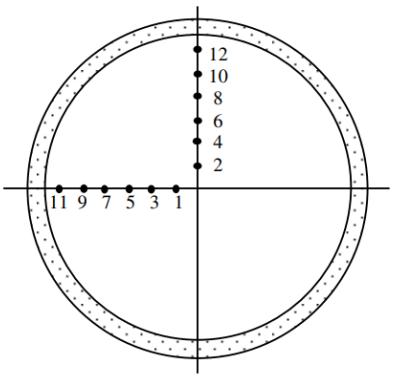

Figure 3. Pressure measurement points at the bottom of the cylinder

Table 1. Coordinates of pressure measurement points at bottom of the cylinder

No	R (mm)
1	30
2	40
3	50
4	60
5	70
6	80
7	90
8	100
9	110
10	120
11	130
12	140

Also, data about the cylinder used in the experiment is given below.

Inside diameter of cylinder (R) : 145 mm
Water height inside cylinder (h_o) : 300 mm
Gravitional Acceleration (g) : 9.81 m/s^2
Rotational speed of electric motor (n) : 1000 rpm
Gear Ratio : 6/31

5. EXPERIMENTAL EQUIPMENT

- Cylinderical container
- Electric Motor
- Reductor
- Manometers

6. EXPERIMENTAL PROCEDURE

A certain height of water in the cylinder is rotated with angular velocity of ω by plate.

After a certain period of time, the movement from the base spreads in the whole liquid and the liquid begins to rotate like a solid body. Meanwhile, pressure is measured from the bottom in the liquid and it is observed that there is a radial distribution in the measurement panel.

1. Record the pressure values in the pressure measurement board in millimeters of water column during the experiment. Compare these values with theoretical values.
2. Find and plot the curve of the free surface using the measured pressure values and compare this curve with the curve obtained theoretically.

Prepare all the results and graphics you find properly in accordance with the experiment writing format. Pay attention to the units. Do not forget to write the units of the results you find. Interpret the difference between the experimental and theoretical values you find.

EXPERIMENT 7

DETERMINATION OF DRAG FORCE ON CYLINDRICAL SURFACES

AIM

The aim of this experiment is to determine the static pressure distribution on the cylinder, the force applied by the fluid on the cylinder and the drag coefficient of the cylinder surface. Experiments will be done with different Reynolds numbers.

EQUIPMENT

An open circuit type wind tunnel is used to perform this experiment. Air enters the tunnel through an area that is properly shaped and covered with a protective grid. The test section of the experiment setup is covered with opaque glass. The dimensions of the test section are 305 mm x 305 mm. Beside test part, there is a diffuser and axial fan. The flow rate at the fan outlet is controlled by the double butterfly valve. The fan works with a sound absorber.

In the test section, there is a total pressure tube, a pitot tube, a 24 incremental water manometer and a cylinder of 305 mm in length with a diameter of 64 mm. The cylinder is placed with pressure measuring tips (taps) (Figure 1).

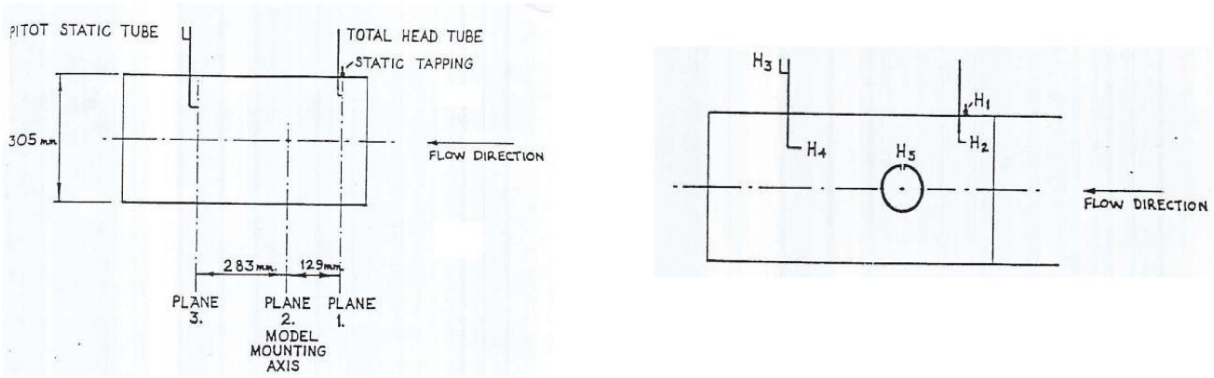

Figure 1. Schematics of the experimental setup

THEORY

As seen in Figure 2, the free flow stops at the stagnation point while pressure increases. After this point, the pressure decreases in the increasing x direction, and the boundary layer develops under a suitable pressure gradient ($dp/dx < 0$). However, the pressure reaches its lowest value at the end of the cylinder, and towards the back of the cylinder, the boundary layer formation is influenced by a pressure gradient in the opposite direction ($dp/dx > 0$). Starting from $u = 0$ at the stagnation point, the flow accelerates with the appropriate pressure gradient ($du/dx > 0$ when $dp/dx < 0$), reaches the highest speed when $dp/dx = 0$, and as a result of the reverse pressure gradient ($du/dx < 0$ when $dp/dx > 0$), slows down. As the fluid slows down, the velocity gradient on the surface $(\partial u/\partial y)_{y=0}$ becomes zero (Figure 3). At this point, referred as the separation point, the fluid near the surface does not have enough momentum to overcome the pressure gradient and downward motion is impossible. Boundary layer separation occurs

because the fluid from behind prevents flow in the reverse direction. At this point, the boundary layer is separated from the surface and a downstream region is formed at the rear. The flow in this region is characterized by vortexes and an irregular flow.

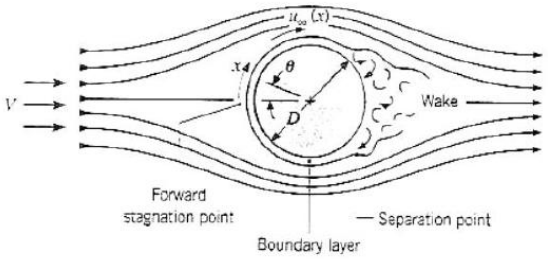

Figure 2. Boundary layer formation and flow separation on a cylindrical surface

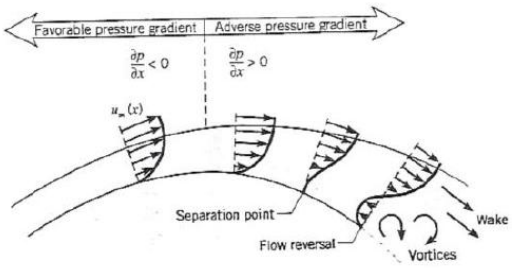

Figure 3. Schematic representation of the boundary layer and velocity profiles in the flow on a cylindrical surface

The transition of the boundary layer, which depends on the Reynolds number, from laminar to turbulence is greatly influenced by the location of the separation point. The characteristic length for the cylinder is the diameter and the Reynolds number is given as,

$$Re_D = \frac{\rho u D}{\mu} = \frac{uD}{\nu} \quad (1)$$

Here, ρ is expressed as the density of the air and its value is 1.24 kg / m^3. The velocity u can be calculated from the Bernoulli equation as follows:

$$u = (2\Delta h / \rho)^{1/2} \quad (2)$$

The measured pressure drop in the wind tunnel is expressed in mmSS.

1 mm H_2O = 9.81 N/m^2

Here, Δh refers to the dynamic pressure and is obtained in the plane 1

$$\Delta h = H_2 - H_1 \quad (3)$$

In the plane number 3,

$$\Delta h = H_4 - H_3 \quad (4)$$

Since the momentum of the fluid in the turbulent boundary layer is greater than the momentum of the fluid in the laminar boundary layer, the transition from laminar to turbulence is expected to delay the separation to a later point. It should be noted that while the friction force value is found for the average velocity value, the blocking effect on the model is allowed to occur. The correction factor for this situation is 1.06.

The above-mentioned phenomena greatly affect the F_D drag force acting on the cylinder. This force has two components. The first one is caused by the boundary layer surface shear stress and is called friction resistance. The other one is related to the pressure difference in the flow direction resulting from the formation of the rear region and is known as shape resistance or pressure resistance. The drag force can be determined as follows;

$$F_3 = (P_3 - P_1)A + \rho A(u_1^2 - u_3^2) \quad (5)$$

Here $P_1 = H_{1g}$ and $P_3 = H_{3g}$ are obtained. After calculating the drag force, the drag coefficient can be calculated as follows;

$$C_D = F_D / A_f (\rho u^2 / 2) \quad (6)$$

Here A_f refers to the projection surface area of the cylinder on the plane perpendicular to the flow (projection area perpendicular to the free flow direction velocity component), and F_D refers to the drag force acting on the cylinder by the fluid.

EXPERIMENTAL PROCEDURE:

Experiments will be carried out to achieve pressure variation along the cylinder surface for different Reynolds numbers. Using the measured pressure values, the drag coefficient, C_D, will be obtained. To complete the experiment, the following operations will be repeated for different speeds (Reynolds number) of the fluid (air).

- Place the cylinder to an inclined position.
- Adjust the double butterfly valve on the out part of the tunnel to provide the desired Reynolds number.
- Rotate the cylinder to measure the pressure values at different points on the cylinder for different inclined positions.
- Repeat the above steps by changing the speed of the air (changing the position of the butterfly valve).

DATA ANALYSIS

1. Draw the pressure distribution around the circular cylinder (a graph for the highest speed value)
2. Plot the variation of pressure distribution H5 with changing θ values around the cylinder and determine the angle of the separation point at the minimum pressure value (draw three lines on a graph)
3. Obtain Equation 5 using basic equations (Momentum and continuity equations).
4. Draw the variation of drag force with Reynolds number.
5. How does the separation angle change with increasing Reynolds numbers?
6. How is the friction and separation values affected by increasing Reynolds number?
7. A large decrease occurs due to the boundary layer transition in the drag force, C_D value. How is the value of separation, rear region and shape resistance affected?
8. Explain whether there is a boundary layer transition.
9. Determine the blockage occurring in the wind tunnel.
10. What happens if the cylinder is larger than 64 mm in diameter?
11. Static pressure is measured by using static pressure tabs or static pressure probe on the wall. What is the difference between these two methods?

SYMBOLS

A	Cross section of the tunnel	m^2
A_f	Front face area of cylinder	m^2
C_D	Drag coefficient	
D	Diameter of the cylinder	m
F_D	Drag force	N
H_1	Static pressure at the entrance to the working area	mmH_2O
H_2	Total pressure at the entrance to the working area	mmH_2O
H_3	Static pressure at the bottom of the model	mmH_2O
H_4	Total pressure at the bottom of the model	mmH_2O
H_5	Static pressure in the pressure tap on the model	mmH_2O
H_θ	Static pressure in rotating the model by the angle θ	mmH_2O
Δh	Dynamic pressure	mmH_2O
Re	Reynolds number for the cylinder	
u	Velocity	m/s
θ	Angle of the cylinder rotated from the pressure tab in the upper position	deg
ρ	Air density	kg/m^3
υ	Kinematic viscosity of air	m^2/s
μ	Dynamic viscosity of air	kg/ms

REFERENCES

1. Incropera, F.P. and Dewitt, D.P., "Introduction to Heat Transfer", Third Edition, John Wiley and Sons, 1996.

2. Fox, R.W. and McDonald, A.T., "Introduction to Fluid Mechanics", Fourth Edition, John Wiley and Sons, 1994.

3. Cengel, Y.A., "Heat Transfer", Mc Graw Hill, 1998.

H_1 =	(mmH_2O)
H_2 =	(mmH_2O)
H_3 =	(mmH_2O)
H_4 =	(mmH_2O)
θ (deg)	H_5 (mmH_2O)
0	
20	
40	
60	
80	
100	
120	
140	
160	
180	

H_1 =	(mmH_2O)
H_2 =	(mmH_2O)
H_3 =	(mmH_2O)
H_4 =	(mmH_2O)
θ (deg)	H_5 (mmH_2O)
0	
20	
40	
60	
80	
100	
120	
140	
160	
180	
200	
220	
240	
260	
280	
300	
320	
340	
360	

H_1 =	(mmH_2O)
H_2 =	(mmH_2O)
H_3 =	(mmH_2O)
H_4 =	(mmH_2O)
θ (deg)	H_5 (mmH_2O)
0	
20	
40	
60	
80	
100	
120	
140	
160	
180	

EXPERIMENT 8
HEAT TRANSFER BY NATURAL CONVECTION

1. INTRODUCTION

In many industrial applications, heat transfer takes place in the form of natural convection. Determining the heat transfer coefficient is very important in these applications in terms of system design.

The purpose of this experiment is investigation of heat transfer in a finned surface which placed on the side face of a vertical channel and determination of heat transfer coefficient on this surface.

2. THEORY

Heat transfer that takes place by temperature difference between a surface and the fluid passing over this surface can be calculated by Newton's law of cooling as,

$$Q = h.A.(T_{surface} - T_{fluid}) \quad (1)$$

Where,

Q: Heat transfer by convection (W),

h: Heat transfer coefficient of the surface (W/m^2K),

A: Heat transfer area ($A = 0{,}13\ m^2$),

$T_{surface}$: Surface temperature (K),

T_{fluid}: Fluid temperature (K).

If heat convection from a surface, surface temperature and fluid temperature are known, the heat transfer coefficient in this surface can be computed by using Equation (1).

3. THE EXPERIMENTAL SETUP

The experimental setup used in this experiment is shown in Figure 1.

The experimental setup consists of a rectangular channel (1), finned plate placed inside the channel (2), and control unit which used for temperature calculations by power control (3). Thermocouples are used to receive the temperature values (4).

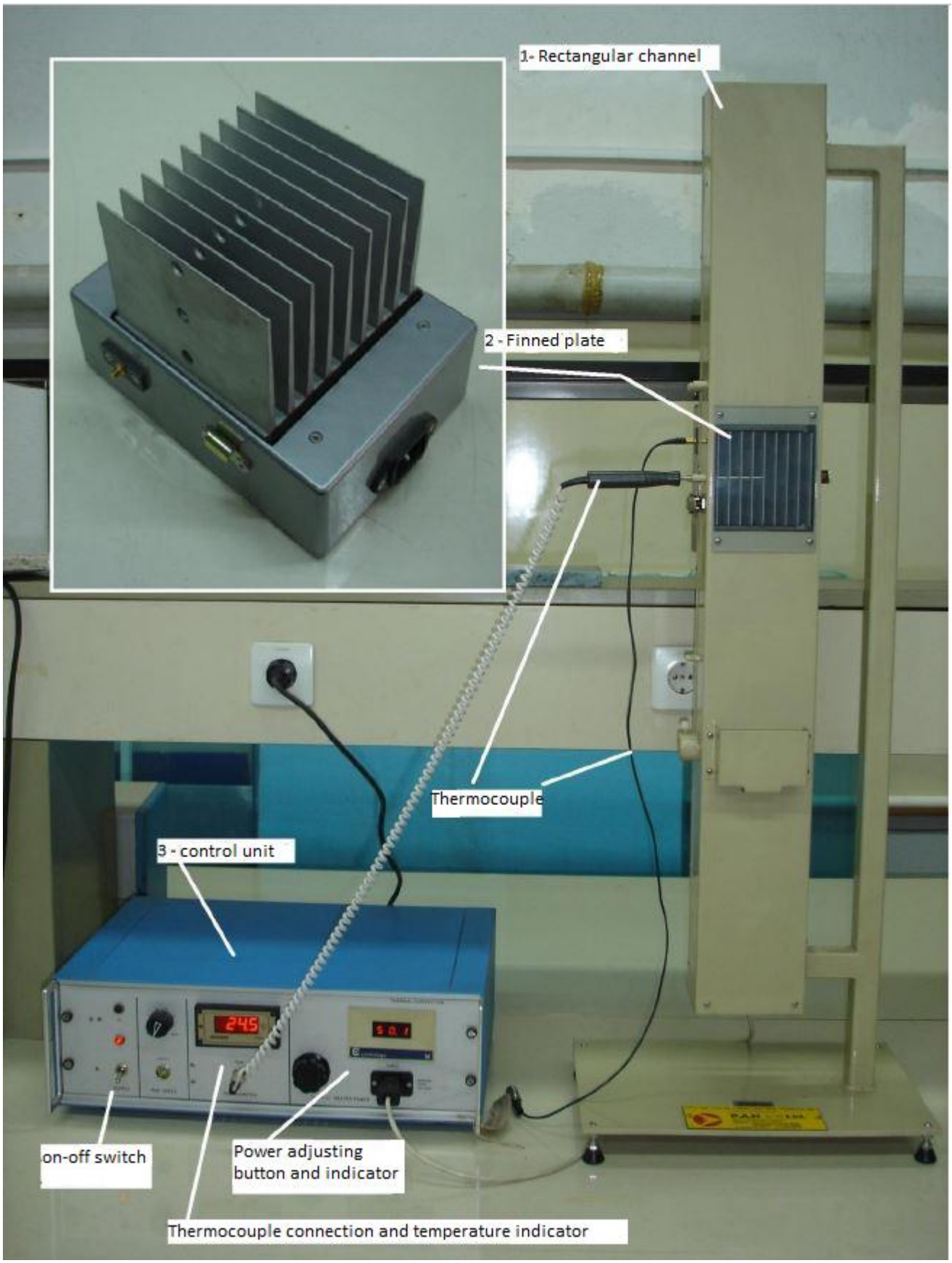

Figure 1. The experimental setup

4. EXPERIMENTAL METHOD

The procedure of experiment is explained below such as:

1. The finned plate is placed in the partition inside the channel and fixed to there.

2. Power connection of the finned plate are made with control unit.

3. The plug of the control unit is connected to the power source and the on-off switch is opened.

4. The power of heater is setted to desired value via the control unit.

5. The surface temperature of the plate is recorded by measuring it periodically, until the system reaches steady conditions. (Appx. 1)

6. After the system reaches steady conditions, temperatures in a,b, and c points are measured. (Appx. 1)

7. The processes explained above, repeated for different heat fluxes.

8. At the end of the experiment,

a. The power unit is unplugged by closing the on-off switch on the control unit.

b. The connection between the power unit and control unit is detached.

c. The finned plate is displaced from the channel.

Note: It is mandatory to obey the electrical safety rules during the experiment. In addition, it is necessary to pay attention to temperatures especially during assembly and disassembly since the fins will get hot.

5. RESULTS

The graphs to be plotted and the calculations to be performed based on the experiment results are specified below:

1. Using the measured temperatures while the system reaches steady-state conditions, plot the Surface Temperature of the Plate vs. Time graph (Appendix 2). (This will be plotted separately for each heat flux.)
2. After the system has reached steady-state conditions, using the measured temperatures, plot the Surface Temperature of the Fins vs. Distance graph (Appendix 3). (This will be plotted separately for each heat flux.)
3. After the system has reached steady-state conditions, using the measured temperatures, calculate the average heat transfer coefficient. (This will be calculated separately for each heat flux.)
4. Plot the Heat Transfer Coefficient vs. Heat Flux graph (Appendix 4).

Appx. 1. Measured Data

Experiment number: Q:				
Time			...	
$T_{surface}$			...	

Experiment nu.	Q	T_{inlet}	$T_{surface}$	T_a	T_b	T_c

Appx. 2.Plate surface temperature – time graph

Appx. 3. Fin surface temperature – distance graph

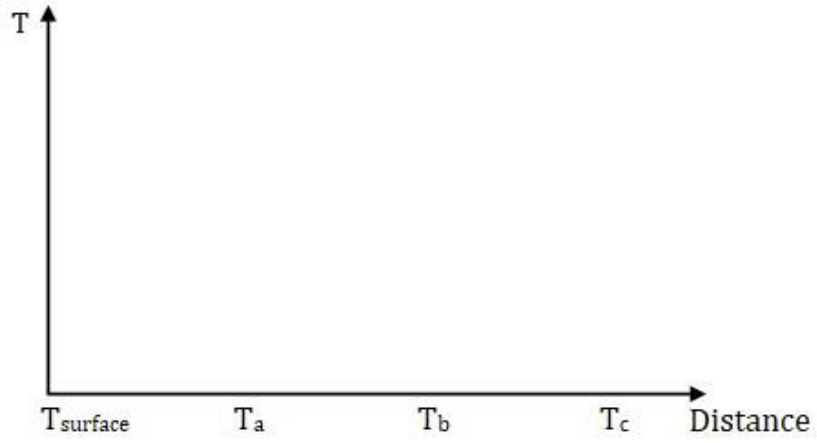

Appx. 4. Heat transfer coefficient – Heat flux graph